Article

A Photoinducible β-Hairpin

Andreas Aemissegger, Vincent Krutler, Wilfred F. van Gunsteren, and Donald Hilvert

J. Am. Chem. Soc., **2005**, 127 (9), 2929-2936• DOI: 10.1021/ja0442567 • Publication Date (Web): 12 February 2005

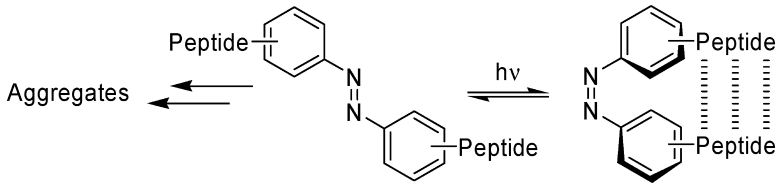

More About This Article

Additional resources and features associated with this article are available within the HTML version:

- Supporting Information
- Links to the 13 articles that cite this article, as of the time of this article download
- Access to high resolution figures
- Links to articles and content related to this article
- Copyright permission to reproduce figures and/or text from this article

View the Full Text HTML

J|A|C|S
ARTICLES
Published on Web 02/12/2005

A Photoinducible β-Hairpin

Andreas Aemissegger,[†] Vincent Kräutler,[‡] Wilfred F. van Gunsteren,[‡] and Donald Hilvert*,[†]

Contribution from the Laboratorium für Organische Chemie and Laboratorium für Physikalische Chemie, Swiss Federal Institute of Technology, ETH-Hönggerberg, CH-8093 Zürich, Switzerland

Received September 21, 2004; E-mail: hilvert@org.chem.ethz.ch

Abstract: A photochromic azobenzene linker was incorporated as a turn element into an amino acid sequence known to fold into a β-hairpin structure in aqueous solution. Oligomer formation when the linker was in its thermodynamically favored trans form prohibited structure determination. Light-induced conformational change of the linker to the cis form led to the formation of monomers which exhibited a well-defined β-hairpin structure as determined by ^{1}H NMR. The rate of the light-induced cis-to-trans isomerization of the azobenzene-containing peptide was 30% slower compared to the unsubstituted chromophore. These results suggest that suitably substituted azobenzenes can be used as photoinducible turn elements to investigate and control the folding and stability of β-sheets.

β-Hairpins are supersecondary structural elements consisting of two adjacent antiparallel peptide strands connected by a short loop. Although such structures often aggregate when removed from their normal tertiary context, model sequences for β-hairpins have been designed over the past decade that fold autonomously in aqueous solution.[1−4] These systems have provided valuable insight into the factors that influence the folding and stability of β-sheet structures, one of the major architectural elements in proteins. They are also useful for probing protein−protein, protein−RNA, and drug−receptor interactions.

The overall stability of β-hairpins is determined by multiple factors. These include interstrand hydrogen bonding, secondary structure propensities of residues in the strands, and side chain−side chain interactions. The loop residues, in particular, have been found to play a crucial role in hairpin folding. For example, the dipeptide ^{L}Asn-Gly, which shows the highest statistical correlation with type I′ β-turns in crystalline structures,[5] is an effective inducer of hairpin structure in short peptides.[6,7] Incorporation of D amino acids at the $i + 1$ residue of the turn is especially beneficial because they intrinsically favor the normal right-handed twist of β-sheets. In fact, the dipeptide ^{D}Pro-Gly has been shown to be superior to ^{L}Asn-Gly in nucleating hairpin formation in aqueous solution,[8] whereas peptidescontaining the enantiomeric ^{L}Pro-Gly are disordered.[9,10] By inserting multiple turn elements into peptides, it has even been possible to construct nonaggregating three- and four-stranded structures.[11,12]

Nonpeptidic elements can also induce antiparallel pairing of peptide strands in water. Successful turn mimics include a variety of conformationally restricted templates, such as dibenzofurans, biphenyls and diphenylacetylenes.[13−16] Photochromic compounds, which undergo large conformational changes when exposed to light of appropriate wavelength, could also be interesting in this context, since they might permit reversible conformational control of hairpin formation.

Of the many photochromic systems that have been described, azobenzenes are potentially well suited for this type of application. They have been extensively characterized, are readily synthesized, and give rise to large changes in the distance between moieties appended to the aryl rings upon interconversion of the trans and thermodynamically less favored cis isomers (Figure 1). Unsubstituted *trans*-azobenzene exhibits three typical absorption bands at 440 nm ($n\rightarrow\pi^*$), 314 nm ($\pi\rightarrow\pi^*$), and 230−240 nm ($\sigma\rightarrow\sigma^*$);[17] substituted compounds have similar spectra with slightly shifted absorption bands (Figure 2). Irradiation at the wavelength of the $\pi\rightarrow\pi^*$ transition converts the trans to the cis isomer, while the reverse process can be achieved either thermally or by irradiation at the wavelength of the $n\rightarrow\pi^*$ transition.

[†] Laboratorium für Organische Chemie.
[‡] Laboratorium für Physikalische Chemie.

(1) Blanco, F.; Ramirez-Alvarado, M.; Serrano, L. *Curr. Opin. Struct. Biol.* **1998**, *8*, 107−111.
(2) Gellman, S. H. *Curr. Opin. Chem. Biol.* **1998**, *2*, 717−725.
(3) Searle, M. S. *J. Chem. Soc., Perkin Trans. 2* **2001**, 1011−1020.
(4) Cochran, A. G.; Skelton, N. J.; Starovasnik, M. A. *Proc. Natl. Acad. Sci. U.S.A.* **2001**, *98*, 5578−5583.
(5) Hutchinson, E. G.; Thornton, J. M. *Protein Sci.* **1994**, *3*, 2207−2216.
(6) de Alba, E.; Jimenez, M. A.; Rico, M. *J. Am. Chem. Soc.* **1997**, *119*, 175−183.
(7) Ramirez-Alvarado, M.; Blanco, F. J.; Serrano, L. *Nat. Struct. Biol.* **1996**, *3*, 604−612.
(8) Stanger, H. E.; Gellman, S. H. *J. Am. Chem. Soc.* **1998**, *120*, 4236−4237.
(9) Haque, T. S.; Gellman, S. H. *J. Am. Chem. Soc.* **1997**, *119*, 2303−2304.
(10) Espinosa, J. F.; Gellman, S. H. *Angew. Chem., Int. Ed.* **2000**, *39*, 2330−2333.
(11) Das, C.; Raghothama, S.; Balaram, P. *Chem. Commun.* **1999**, 967−968.
(12) Schenck, H. L.; Gellman, S. H. *J. Am. Chem. Soc.* **1998**, *120*, 4869−4870.
(13) Diaz, H.; Espina, J. R.; Kelly, J. W. *J. Am. Chem. Soc.* **1992**, *114*, 8316−8318.
(14) Diaz, H.; Kelly, J. W. *Tetrahedron Lett.* **1991**, *32*, 5725−5728.
(15) Diaz, H.; Tsang, K. Y.; Choo, D.; Kelly, J. W. *Tetrahedron* **1993**, *49*, 3533−3545.
(16) Kemp, D. S.; Li, Z. Q. *Tetrahedron Lett.* **1995**, *36*, 4175−4178.
(17) Griffiths, J. *Chem. Soc. Rev.* **1972**, *1*, 481−493.

10.1021/ja0442567 CCC: $30.25

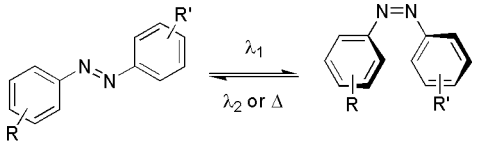

	R	R'
2a	*o*-CH_2CO_2H	*o*-CH_2NH_2
2b	*m*-CH_2CO_2H	*m*-CH_2NH_2
2c	*p*-CH_2CO_2H	*p*-CH_2NH_2

Figure 1. Cis−trans isomerization of azobenzene.

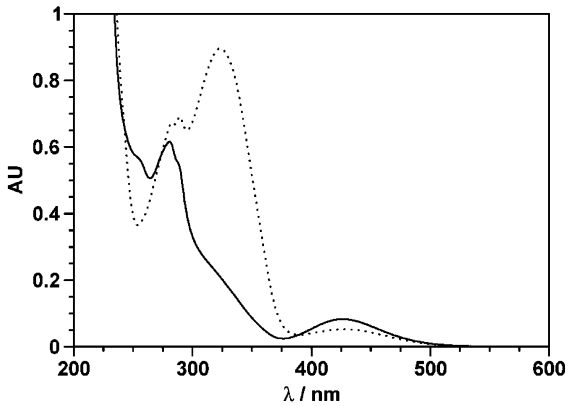

Figure 2. Absorption spectra for **1b** in the thermodynamic (···) and photostationary (—) state. The maxima for the $\pi\rightarrow\pi^*$ and $n\rightarrow\pi^*$ transitions are at 314 and 426 nm, respectively.

These properties have already been extensively exploited to photoregulate the conformation of crown ethers[18] and cyclodextrins[19] and the permeability of membranes.[20,21] Azobenzene chromophores have also been introduced into peptides and proteins, both in side chains[22−25] and in the backbone.[26−28] The ability of an azobenzene to template a β-turn conformation in a cyclic peptide when in its cis form is particularly notable in the present context.[26] Here we show that azobenzenes can also serve as photoswitchable β-turn mimics in open chain polypeptides, providing excellent conformational control in aqueous solution.

Results

Peptide Design. The 12-residue peptide **1a** (Scheme 1) derived from protein GB1 has been shown by Gellman and coworkers to adopt a hairpin structure in aqueous solution.[10] The ^{D}Pro-Gly segment at positions 6 and 7 nucleates hairpin formation and was targeted for replacement by an azobenzene-containing turn mimetic. Favorable interactions between the hydrophobic cluster formed by the aromatic side chains and the turn element in its cis configuration were anticipated to favor a well-defined hairpin structure.

Scheme 1 [a]

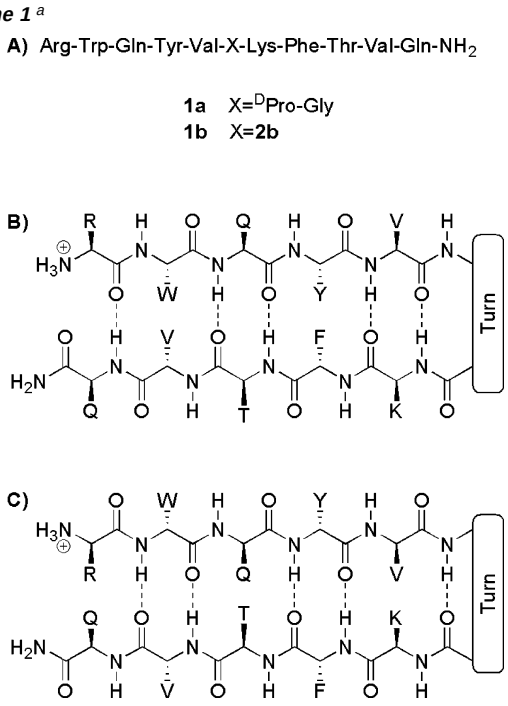

[a] (A) Model hairpin sequences with turn element X. (B and C) Possible hydrogen bonding patterns for the β-hairpin. Structural data for peptide **1a** is consistent with the pattern shown in B, whereas the azobenzene-containing peptide *cis*-**1b** is better described by pattern C (see text).

Azobenzene units which have been previously incorporated into peptide backbones generally contain *p*-substituted aryl rings.[26−28] However, visual inspection of models suggested that this substitution pattern might not be optimal for a turn mimetic. All possible symmetrical substitution patterns (Figure 1) were therefore investigated by molecular dynamics (MD) simulation with respect to their ability to template hairpin formation.[29] Additionally, one and two methylene groups were allowed as spacers between the functional groups and the aryl rings to accommodate interstrand interactions between the appended peptides.[29]

The MD simulations indicated that amino acid **2b**, with *meta*-substituted aryl rings and a single methylene group spacer, was one of the most promising turn mimetics. Because the substituents are not in conjugation with the central N=N bond, thermal cis−trans isomerization of *meta*-substituted azobenzenes should be substantially slower than for *para*-substituted azobenzenes.[30] This configurational stability was expected to be advantageous for structural investigations by NMR spectroscopy.

Synthesis. As described for similar compounds,[31] the synthesis of **10** relies on the reaction of a nitrosobenzene **5** with an aniline **8** (Scheme 2). Compound **5** was prepared by esterification of commercially available *m*-nitrophenylacetic acid **3** under Mukaiyama conditions,[32] followed by reduction of the nitro group to the hydroxylamine with Zn dust in NH_4Cl solution and immediate reoxidation with $FeCl_3$ to the nitroso compound.

(18) Shinkai, S.; Manabe, O. *Top. Curr. Chem.* **1984**, *121*, 67−104.
(19) Ueno, A.; Tomita, Y.; Osa, T. *Tetrahedron Lett.* **1983**, *24*, 5245−5248.
(20) Kano, K.; Tanaka, Y.; Ogawa, T.; Shimomura, M.; Okahata, Y.; Kunitake, T. *Chem. Lett.* **1980**, 421−424.
(21) Kano, K.; Tanaka, Y.; Ogawa, T.; Shimomura, M.; Kunitake, T. *Photochem. Photobiol.* **1981**, *34*, 323−329.
(22) Pieroni, O.; Houben, J. L.; Fissi, A.; Costantino, P. *J. Am. Chem. Soc.* **1980**, *102*, 5913−5915.
(23) Willner, I.; Rubin, S. *React. Polym.* **1993**, *21*, 177−186.
(24) Liu, D.; Karanicolas, J.; Yu, C.; Zhang, Z. H.; Woolley, G. A. *Bioorg. Med. Chem. Lett.* **1997**, *7*, 2677−2680.
(25) Kumita, J. R.; Smart, O. S.; Woolley, G. A. *Proc. Natl. Acad. Sci. U.S.A.* **2000**, *97*, 3803−3808.
(26) Ulysse, L.; Cubillos, J.; Chmielewski, J. *J. Am. Chem. Soc.* **1995**, *117*, 8466−8467.
(27) Renner, C.; Behrendt, R.; Sporlein, S.; Wachtveitl, J.; Moroder, L. *Biopolymers* **2000**, *54*, 489−500.
(28) Renner, C.; Cramer, J.; Behrendt, R.; Moroder, L. *Biopolymers* **2000**, *54*, 501−514.
(29) Kräutler, V.; Aemissegger, A.; Hünenberger, P. H.; Hilvert, D.; Hansson, T.; van Gunsteren, W. F. *J. Am. Chem. Soc.*, in press.
(30) Asanuma, H.; Liang, X. G.; Komiyama, M. *Tetrahedron Lett.* **2000**, *41*, 1055−1058.
(31) Ulysse, L.; Chmielewski, J. *Bioorg. Med. Chem. Lett.* **1994**, *4*, 2145−2146.
(32) Saigo, K.; Usui, M.; Kikuchi, K.; Shimada, E.; Mukaiyama, T. *Bull. Chem. Soc. Jpn.* **1977**, *50*, 1863−1866.

Scheme 2 [a]

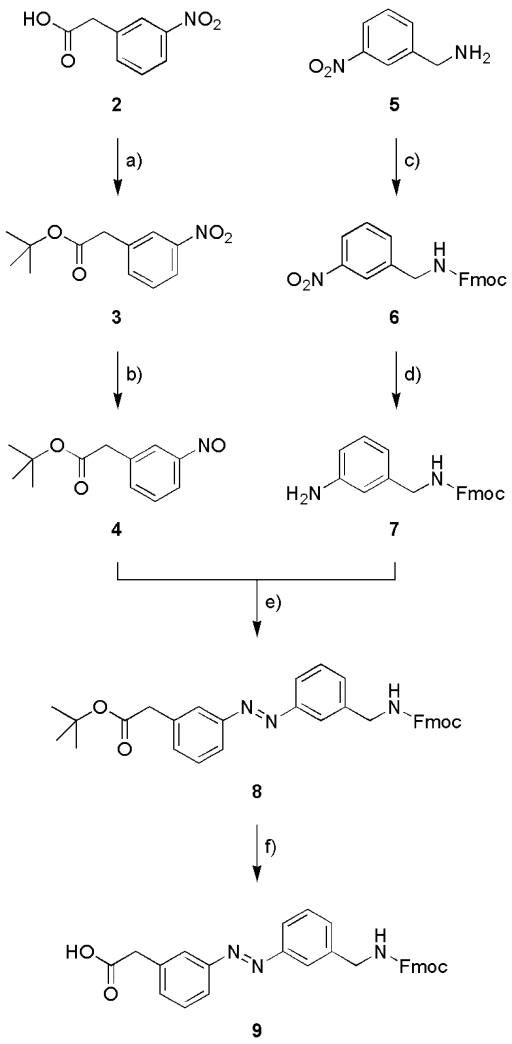

[a] Conditions: (a) ^{t}BuOH, 2-chloro-1-methylpyridinium iodide, Bu_3N; (b) NH_4Cl, Zn, then $FeCl_3$; (c) Fmoc-Cl, Hünig's base; (d) H_2, PtO_2; (e) AcOH; (f) TFA, CH_2Cl_2

Aniline **8** was obtained from commercially available 3-nitrobenzylamine hydrochloride **6** via a two-step sequence, involving introduction of an Fmoc protecting group followed by reduction of the nitro group. Although catalytic reduction by palladium on charcoal leads to partial deprotection of the amine, **8** was obtained in quantitative yield using PtO_2 instead. Coupling of **5** and **8** in glacial acetic acid afforded the fully protected azobenzene amino acid **9** in 57% yield. Cleavage of the *tert*-butyl ester group with TFA in dichloromethane gave the turn mimetic **10** in a form suitable for standard Fmoc solid-phase peptide synthesis.

The synthesis of the azobenzene-containing peptide **1b** was carried out on a 0.1 mmol scale using standard conditions (20% piperidine in DMF for Fmoc deprotection, HOBt/HBTU for activation, diisopropylethylamine as base, and *N*-methylpyrrolidinone as solvent) on a Rink amide resin. The peptide was cleaved from the resin with TFA/H_2O/TIPS 93:5:2 and purified by reversed-phase HPLC.

Biophysical Characterization. As judged by analytical HPLC, 90% of peptide **1b** has a trans configuration at thermodynamic equilibrium; 10% adopts the cis configuration. The cis content increases to about 85% in the photostationary state. Irradiation of the peptide in a Rayonet photoreactor equipped with RPR-3500 lamps and separation of the two isomers by preparative HPLC afforded the cis isomer in greater than 98% purity.

Analytical ultracentrifugation at 4 °C shows the cis isomer to be monomeric with an apparent molecular weight of 1688 ± 48 Da, in good agreement with the calculated molecular weight of 1604 Da considering the error introduced by modeling the azobenzene unit as two phenylalanines in the calculation of the partial specific volume of the peptide. When the temperature of the rotor was raised to 40 °C, the absorption intensity gradually decreased (data not shown) due to precipitation of the trans isomer that is formed upon thermal isomerization of the sample.

The rate of the cis to trans isomerization of peptide **1b** was determined by monitoring the increase in the $\pi\rightarrow\pi^*$ absorption band at 323 nm. To assess the influence of the peptide on the isomerization, compound **2b** was studied under identical conditions. The latter was prepared by treating **10** with 20% piperidine in DMF for 1 h and purification by analytical HPLC. Irradiation in the Rayonet photoreactor gave the cis form of the water soluble amino acid in >90% purity as judged by analytical HPLC. Because the dark reaction of azobenzenes is strongly dependent on the pH,[33−38] the reactions were carried out in 20 mM acetate buffer at pH 3.8. In the absence of light at 25 °C, peptide **1b** and amino acid **2b** thermally isomerize with a rate constant of about 5×10^{-7} s^{-1}, corresponding to a half-life of >2 weeks. Photoisomerizations were carried out at 25 °C at 431 and 420 nm for the cis peptide and **2b**, respectively. A rate constant of $(1.5 \pm 0.1) \times 10^{-4}$ s^{-1} was obtained for the peptide, which can be compared to a value of $(2.2 \pm 0.5) \times 10^{-4}$ s^{-1} for the amino acid alone.

NMR Experiments. The trans form of peptide **1b** forms a highly viscous solution at 4 °C at a concentration of 9 mg/mL (5.6 mM). The NMR spectrum of this sample shows extensive signal broadening (Figure 3A), most likely due to extensive aggregation of the peptide. Four-fold dilution of the sample and increasing the temperature to 25 °C allowed a reasonably well-resolved 1D proton spectrum to be recorded. However, significant noise in the 2D spectra and the presence of 10% of the peptide containing the cis form of the linker precluded assignment of peaks to residues and determination of a three-dimensional structure.

In contrast, the cis form of the peptide dissolves readily at a concentration of 5.8 mg/mL (3.6 mM) and yielded spectra with sharp and well resolved signals at 4 °C (Figure 3B). A full set of DQF-COSY, TOCSY, and NOESY spectra was recorded. UV data showed that thermal isomerization was negligible for the duration of the NMR analysis (data not shown).

Resonance Assignment and Structure Determination. Numerous NOE signals between residues that are not adjacent in sequence are evident in the spectra of cis peptide **1b** (see Supporting Information for a full list of chemical shifts and NOE

(33) Sokalski, W. A.; Gora, R. W.; Bartkowiak, W.; Kobylinski, P.; Sworakowski, J.; Chyla, A.; Leszczynski, J. *J. Chem. Phys.* **2001**, *114*, 5504−5508.
(34) Sanchez, A. M.; Barra, M.; de Rossi, R. H. *J. Org. Chem.* **1999**, *64*, 1604−1609.
(35) Sanchez, A. M.; de Rossi, R. H. *J. Org. Chem.* **1995**, *60*, 2974−2976.
(36) Lovrien, R.; Pesheck, P.; Tisel, W. *J. Am. Chem. Soc.* **1974**, *96*, 244−248.
(37) Wettermark, G.; Langmuir, M. E.; Anderson, D. G. *J. Am. Chem. Soc.* **1965**, *87*, 476−481.
(38) Lovrien, R.; Waddington, J. C. *J. Am. Chem. Soc.* **1964**, *86*, 2315−2322.

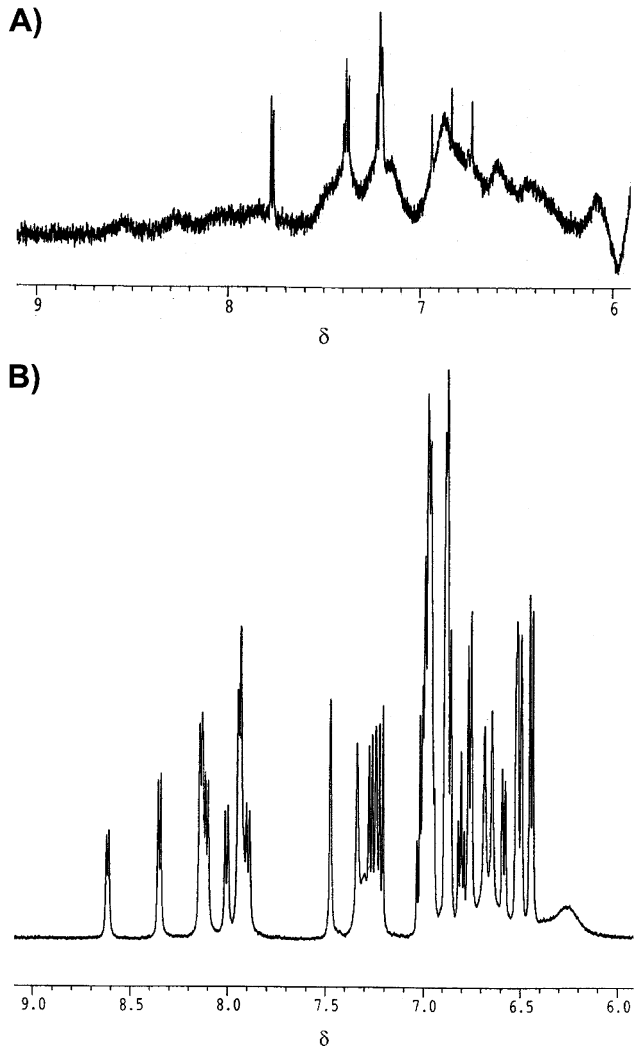

Figure 3. ^{1}H NMR spectra of peptide **1b** in 1:9 D_2O/H_2O 50 mM sodium acetate buffer pH 3.6, 4 °C. (A) *trans*-**1b** at 5.6 mM, (B) *cis*-**1b** at 3.6 mM

resonance assignments). Although multiple NOE signals involving the ring protons of the azobenzene and F8 residues could not be assigned unambiguously, a total of 53 other NOE distance restraints were available for structure calculations. These included strong intra- and interstrand signals. Simulated annealing was performed with the program CNS.[39]

A total of 100 structures was generated from the NMR data. The superposition of the 10 best structures (as judged by the lowest overall energies) indicates that the peptide forms a hairpin structure which has considerable flexibility at its termini and also in the turn region (Figure 4A). In addition, the C-terminal strand appears to be somewhat more flexible than its N-terminal counterpart. Explicit solvent MD simulations were used for further refinement of the structure to accommodate solvent and electrostatic effects.[29] Analysis of the resulting structures (Figure 5) revealed that two NOE distance restraints are incompatible with the calculated structures. Both of these violations involve the amide proton of residue F8. Reexamination of the NOESY peak assignments showed an ambiguity and likely misassignment in one of these cases, which occurs at the intersection of

(39) Brunger, A. T.; Adams, P. D.; Clore, G. M.; DeLano, W. L.; Gros, P.; Grosse-Kunstleve, R. W.; Jiang, J.-S.; Kuszewski, J.; Nilges, N.; Pannu, N. S.; Read, R. J.; Rice, L. M.; Simonson, T.; Warren, G. L. *Acta Crystallogr.* **1998**, *D54*, 905−921.

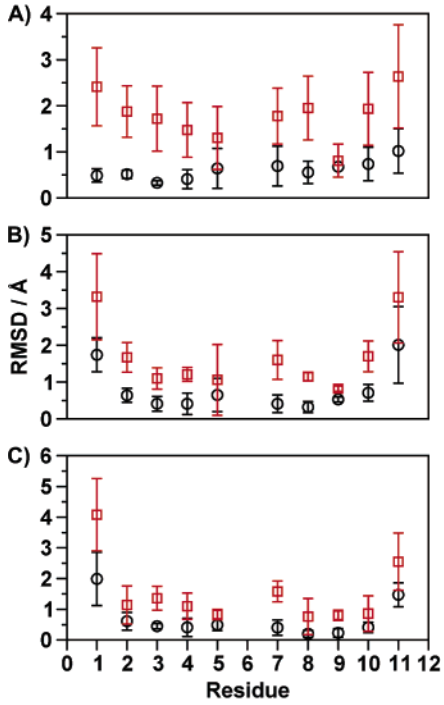

Figure 4. RMSD values for backbone (○) and side chain (□) atoms for the structures obtained by simulated annealing with respect to their average structure. (A) Originally calculated structure based on all NOE restraints, including the two misassigned values. (B and C) Clusters 1 and 2 obtained after removal of the erroneous NOEs.

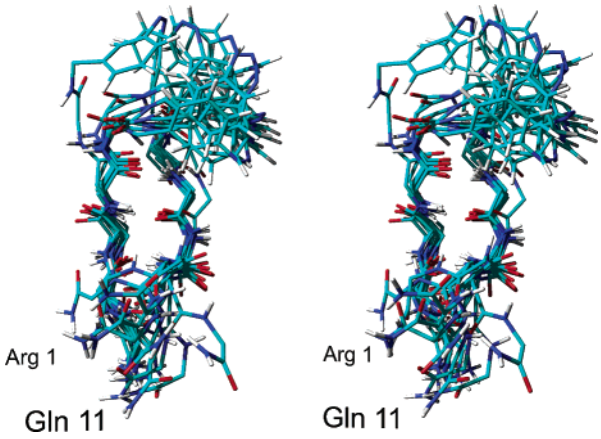

Figure 5. Cross-eyed stereo superposition of the 10 best structures (backbone atoms only) of the primary cluster (87% of the trajectory) obtained in the explicit solvent MD simulation of peptide *cis*-**1b**.

two regions of nearly isochronous nuclei. As numerous NOEs are observed between the side chains of residues W2 and Y4, and residue Y4 shows a relatively strong NOE to the amide proton of residue F8, the other restraint in question is most likely the result of spin diffusion. This conclusion is supported by the observation that this NOE is only present in the 400 ms NOESY spectrum.

In the originally generated structures the side chain of residue T9 has an anomalously low RMSD value compared to the other amino acids in the peptide, suggesting that it is strongly constrained (Figure 4A). However, this result appears to be an artifact that arose because the two problematic NOEs were included in the calculations. When the refinement was repeated without them, a new set of 100 structures was obtained which are evenly divided into two clusters of hairpins (Figure 6), each

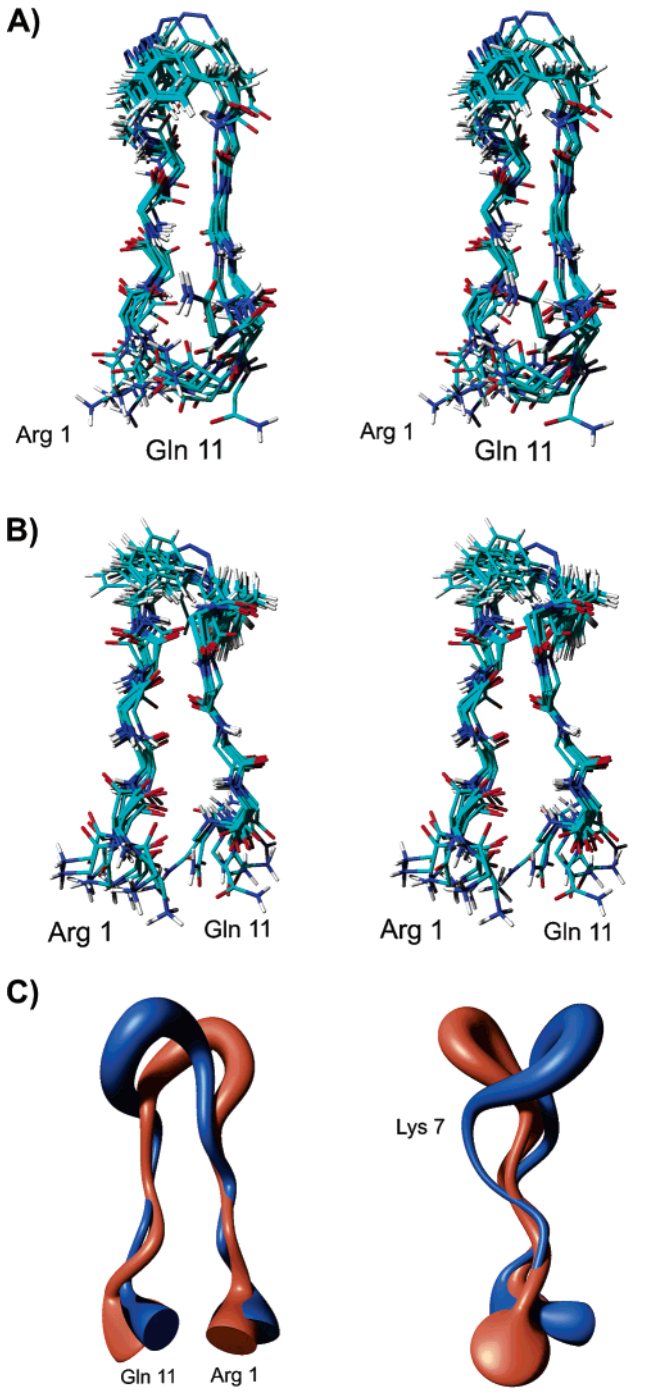

Figure 6. (A and B) Cross-eyed stereo superposition of the 10 best structures (backbone atoms only) of the two clusters obtained by simulated annealing of peptide *cis*-**1b**. (C) Superposition of the polypeptide backbone for best fit of the backbone heavy atoms for residues 2−5 and 7−10. The radius of the cylindrical rods representing the polypeptide chains is proportional to the mean backbone displacement per residue among the 10 lowest energy conformers of each cluster. The two representations differ by a 90° rotation about the vertical axis.

containing approximately 45% of all structures, plus a variety of outliers. None of the outliers is among the 50 best (lowest overall energy) structures. The two main clusters do not differ significantly in terms of overall energy. The per-residue RMSDs observed for the side chain of residue T9 in the new structures are in the range of the adjacent amino acids (Figure 4B and 4C). Additionally, the orientation of the side chains is much better defined. Whereas the ensemble of 10 lowest energy structures from the initial calculation had an average RMSD to the mean coordinates of 0.66 ± 0.22 Å for the backbone atoms of all residues except the linker and 1.65 ± 0.35 Å for all heavy atoms, these values dropped to 0.55 ± 0.19 Å/0.43 ± 0.17 Å for the backbone and 1.17 ± 0.28 Å/0.99 ± 0.26 Å for the side chains of cluster 1/cluster 2. For the latter calculations, the N- and C-terminal residues were excluded as they are heavily disordered.

Discussion

The properties of peptide **1b** establish the feasibility of using azobenzene chromophores as photoswitches to control the conformation of open chain polypeptides in aqueous solution. In its cis configuration, the *meta*-substituted azobenzene mimics the dipeptide ^{D}Pro-Gly in nucleating a stable and monomeric hairpin structure. In contrast, the trans configured peptide does not adopt a unique structure in accord with MD simulations[29] and tends to form higher order aggregates. Until the latter ultimately precipitate from solution, the peptide can be reversibly switched between the cis and trans states by irradiation at an appropriate wavelength.

The structure deduced for *cis*-**1b** is an ensemble of hairpins with a well-defined stem and the expected residue pairings. In addition to the usual flexibility at the N- and C-termini, the linker appears to be considerably more mobile than conventional type I′ and II′ turns, which are strongly constrained by hydrogen bonds between the first and fourth residues of the turn. Two major, roughly isoenergetic conformations are evident that differ with respect to the orientation of the azobenzene linker either above or below the plane of the hairpin (Figure 6C). Additionally, although steric clashes prevent the aromatic rings from simultaneously occupying the plane of the cis configured N−N double bond, rotation around the C−N bond allows them to explore multiple conformational states. The methylene spacers at the meta positions of the azobenzene appear to insulate the peptide strands somewhat from the linker so that only the immediately flanking residues are affected by its flexibility. Thus, the backbone conformation of the peptide strands in an overlay of the 10 best structures from each cluster is strikingly similar, with only residue K7 showing a significant displacement due to the different azobenzene conformations (Figure 6C). The side chains of residues 2 to 4 and 8 to 10 are completely unaffected by linker flexibility and maintain essentially identical packing in the two primary clusters.

Aside from differences in the turn region, the hairpin structures deduced for *cis*-**1b** qualitatively resemble those reported for **1a**. Nevertheless, there is one important difference. In **1a**, strong backbone−backbone NOEs were observed between the Hα protons of residues W2 and V11 (corresponding to W2 and V10 in peptide **1b**) and Y4 and F9 (corresponding to Y4 and F8).[10,40] These are missing in *cis*-**1b**. Instead, a strong NOE between Hα of residue Q3 and HN of residue T9 is observed. This result indicates that the backbones of the N- and C-strand segments are both flipped by ca. 180° so that the Hα protons which face the opposite strand in one peptide are directed toward the surrounding solvent in the other (Scheme 1B versus 1C).

(40) Espinosa, J. F.; Syud, F. A.; Gellman, S. H. *Protein Sci.* **2002**, *11*, 1492−1505.

Although **1a** and *cis*-**1b** exhibit different interstrand hydrogen bonding patterns, the hydrophobic side chains of W2, Y4, F8, and V10 cluster similarly in both. This hydrophobic core is believed to contribute to the stability of **1a** in aqueous solution[10] and likely plays a similar role in the azobenzene-containing peptide. Moreover, investigations of dibenzofuran- and biphenyl-type turn templates have shown that hydrophobic interactions between the β-turn mimic and the side chains of amino acids on one face of the hairpin can further stabilize sheetlike structures in solution.[41−43] Analogous interactions are evident between the four hydrophobic residues and the photochromic linker in one of the structure clusters obtained in the simulated annealing calculations. In the second cluster, the azobenzene bends to the opposite face of the sheet toward the hydrophobic side chain of V5.

NOE intensities were previously used to estimate that 50 to 75% of peptide **1a** adopts the β-hairpin fold at 3 °C.[10] The extent of β-hairpin folding in the azobenzene-containing *cis*-**1b** cannot be reliably estimated using the same NOE-based analysis because it assumes a two state model in which the peptide is either folded, so that interproton distances are well defined and correlate with signal intensity, or unfolded, in which case the protons are too far apart to give rise to an NOE. This two state assumption is questionable if a preorganizing turn element forces the two short peptide strands into a specific orientation, as is the case here. In principle, Hα chemical shifts offer an alternative method of quantifying populations, as they are highly sensitive to local secondary structure.[44−46] However, reference values are required for the fully folded and unfolded states, as equilibration is rapid on the NMR time scale. Unfortunately, the unfolded state of **1b**, as modeled by the trans form, produces aggregates, precluding collection of relevant NMR data. Although we have not been able to reliably quantify the fraction of the *cis*-**1b** peptide populating the β-hairpin, the population of compact structures is likely to be comparable to that observed for **1a** based on the quality of the spectra, which show no other species, the absence of aggregation even after several weeks, and the preorganizing nature of the *cis*-configured chromophore.

Unrestrained MD simulations with a physically meaningful force field and explicit solvent were employed to provide a more realistic assessment of the solution structure of the peptide.[29] The conventional in vacuo simulated annealing process, which was utilized to determine the structures described above, only considers bonded and repulsive van der Waals interactions. While this method predicts a well-defined hairpin structure for *cis*-**1b**, it neglects electrostatic, hydrophobic, and solvent effects that undoubtedly influence the ensemble of accessible conformations accessible to the peptide in aqueous solution. As noted above, hydrophobic interactions are likely to be extremely important in this system.

Starting either from the initially generated NMR model or from a fully extended structure, the MD simulations converged to a stable β-hairpin that is consistent with all the experimental data (Figure 5). In agreement with the simulated annealing results, the peptide strands are packed differently than in the hairpin formed by parent peptide **1a**,[10,40] favoring the hydrogen bonding arrangement shown in Scheme 1C over that in Scheme 1B. In contrast to the in vacuo calculations, however, only a single family of structures is observed. The azobenzene unit appears to be highly mobile and folds toward the hydrophobic residues W2, Y4, F8, and V10 as seen in one of the clusters obtained by simulated annealing. In the explicit solvent MD simulation, the hydrophobic core formed by W2, Y4, and V10 is more compact than in the structures obtained by simulated annealing. Moreover, the unrestrained MD simulation places F8 and the turn element in close contact, a finding that is supported by the numerous NOE signals involving the turn element and residue F8 that were observed but could not be assigned unambiguously. The interaction between F8 and the chromophore favors the right-handed twist commonly observed for β-sheets embedded in proteins (Figure 5).[47]

In summary, we have prepared an Fmoc-protected azobenzene amino acid **10** that is compatible with solid-phase synthesis and can be readily incorporated into peptides. Our results show that its insertion into the backbone of a short open chain polypeptide enables reversible control of peptide conformation in solution. Like the central dipeptide in a conventional β-turn, this chromophore is able, in its cis configuration, to preorganize two peptide strands as a β-hairpin. In the specific case examined, the azobenzene is much floppier than a dipeptide turn element and favors a different set of interactions between the attached strands. Nevertheless, based on its ability to organize the side chains of a polypeptide spatially, this turn mimic could prove useful as a photoregulatory element to control β-hairpin formation in peptide hormones or larger proteins, including enzymes.

Materials and Methods

Materials. All commercially available reagents and solvents were used as received. Organic extracts were dried over magnesium sulfate, filtered, and concentrated using a rotary evaporator. Nonvolatile oils and solids were dried under vacuum at 0.01 Torr. Reactions were monitored by thin-layer chromatography on precoated E. Merck silica gel 60 F254 plates (0.25 mm) and visualized either by short wave UV or by staining with 10% ethanolic phosphomolybdic acid. Flash chromatography was performed on Fluka silica gel 60. Chemical shifts are expressed in ppm relative to tetramethylsilane or the solvent signal. All melting points are uncorrected.

General Methods. UV irradiation was carried out in a Rayonet photoreactor using 350 nm fluorescent tubes or in an Aviv 202 CD spectrometer at the desired wavelength with a bandwidth of 10 nm. Irradiated peptides were handled in dimmed light and stored at −80 °C. Sedimentation equilibrium analysis was performed in a Beckman Optima XL-A analytical ultracentrifuge with an An60Ti rotor at three different rotor speeds at 4 °C in 10 mM acetate buffer, pH 3.8 with 90 mM NaCl. Observed molecular weights were determined using the Ultrascan II package.[48] The partial specific volume was calculated from the amino acid composition, substituting the azobenzene linker by two phenylalanine residues.

Peptide Synthesis. Peptide synthesis was carried out on a 0.1 mmol scale using standard Fmoc chemistry on a Rink amide resin (loading

(41) Schneider, J. P.; Kelly, J. W. *Chem. Rev.* **1995**, *95*, 2169−2187.
(42) Nesloney, C. L.; Kelly, J. W. *J. Am. Chem. Soc.* **1996**, *118*, 5836−5845.
(43) Nesloney, C. L.; Kelly, J. W. *J. Org. Chem.* **1996**, *61*, 3127−3137.
(44) Wishart, D. S.; Sykes, B. D.; Richards, F. M. *J. Mol. Biol.* **1991**, *222*, 311−333.
(45) Wishart, D. S.; Sykes, B. D.; Richards, F. M. *Biochemistry* **1992**, *31*, 1647−1651.
(46) Williamson, M. P. *Biopolymers* **1990**, *29*, 1428−1431.
(47) Chothia, C. *J. Mol. Biol.* **1973**, *75*, 295−302.
(48) Demeler, B. *Ultrascan II*, version 6.2; The University of Texas: San Antonio.

0.54 mmol/g) on an Applied Biosystems 432A peptide synthesizer. Cleavage from the resin and amino acid side chain deprotection was done with a mixture of 2% triisopropylsilane and 5% H_2O in TFA for 40 min and subsequent precipitation of the crude peptide from cold diethyl ether. The peptide was purified by preparative reversed-phase HPLC (Nucleosil 100-7 C18 250 × 21 mm^2, 5% to 60% acetonitrile over 45 min in water containing 0.1% trifluoroacetic acid at a flow rate of 10 mL/min), and purity of the isolated isomers was confirmed by analytical HPLC (Nucleosil 100−5 C18 250 × 4.6 mm^2, 5% to 60% acetonitrile containing 0.05% TFA over 45 min in water containing 0.1% TFA at a flow rate of 1 mL/min.). Retention times for cis and trans were 29.7 and 31.5 min, respectively. ESI MS *m*/*z* M^+ calcd 1604.9, found 1604.9.

NMR Spectroscopy. NMR experiments involving peptides were carried out at 25 °C (trans) or 4 °C (cis) in 1:9 D_2O/H_2O 50 mM sodium acetate buffer pH 3.8 (uncorrected) on a Bruker DRX 500. The solvent signal was suppressed by a 2 s presaturation delay. All 2D spectra were recorded with 512 increments in F1 (TPPI) and 4k data points in F2. These were processed to 1k data points in F1 and F2 with a $\cos^2$ filter in F1 and a $\cos^2$ filter shifted by $\pi/3$ in F2. For phase sensitive DQF-COSY, 32 scans per FID were recorded. For TOCSY, 48 scans per FID were recorded with a 9 kHz spin lock (DIPSY2) and a mixing time of 80 ms. For NOESY, 64 scans per FID were recorded with mixing times of 100 and 400 ms, respectively.

Hβ1-Hβ2 and Hε1-Hζ2 cross-peaks of F8 and W2, respectively, were used as reference for NOE intensities. Peak assignments were done with Sparky[49] and initial structures were calculated via torsion angle dynamics using CNS.[39]

Kinetic Measurements. Isomerization kinetics were performed by irradiating purified *trans*-**1b** in an Aviv 202 CD spectrometer at 320 nm with a bandwidth of 10 nm until the photostationary state was reached. The isomerization back to *trans*-**1b** was then monitored by UV using thermostated samples stored in the dark or with irradiation at 420 nm. Rate constants were derived by fitting the data to a first-order process.

MD Simulations. MD simulations were performed using the GROMOS96 program,[50,51] with the GROMOS 43A1 united-atom force field[51] and the SPC water model.[52] Parameter details are published elsewhere.[29]

3-Nitrophenylacetic Acid *tert*-Butyl Ester (4). A solution of 4.95 g (27.4 mol) of 3-nitrophenylacetic acid, 2.06 g (27.9 mmol) of *tert*-butanol, and 16 mL (66.8 mmol) of tributylamine in 100 mL of toluene was added to a suspension of 8.45 g (33.0 mmol) of 2-chloro-1-methylpyridinium iodide in 50 mL of toluene. The mixture was refluxed overnight. After removal of the solvent, the dark residue was purified by flash chromatography (EtOAc/hexane 1:3) to obtain 5.73 g (88%) of a pale yellow oil. ^{1}H NMR ($CDCl_3$, 400 MHz): δ 8.16 (s, 1 H), 8.13 (d, J = 8.1 Hz, 1 H), 7.62 (d, J = 8.1 Hz, 1 H), 7.50 (t, J = 7.9 Hz, 1 H), 3.65 (s, 2 H), 1.46 (s, 9 H). ^{13}C NMR ($CDCl_3$, 100 MHz): δ 169.6, 148.3, 135.6, 129.3, 124.4, 122.1, 81.75, 42.0, 28.0. MS (EI) *m*/*z* 237.2. Elemental analysis $C_{12}H_{15}NO_4$, calcd: C, 60.75; H, 6.37; N, 5.90. Found: C, 60.81; H, 6.45; N, 6.01.

3-Nitrosophenylacetic Acid *tert*-Butyl Ester (5). To a solution of 5.73 g (24.2 mmol) of **4** in 200 mL of methoxyethanol was added a solution of 1.9 g (35.6 mmol) of NH_4Cl in 50 mL of H_2O. The solution was thoroughly degassed by bubbling a stream of argon through it for about 30 min. A total of 4 g of Zn dust was added very slowly. The reaction mixture was stirred for 6 h at room temperature, filtered, and slowly added to a solution of 12.4 g (48.9 mmol) of $FeCl_3 \cdot 6\ H_2O$ in a 2:1 mixture of H_2O and EtOH at −10 °C. After 1 h the mixture was allowed to warm to room temperature and stirred for another hour. It was extracted 3 times with EtOAc, the organic extracts were dried over $MgSO_4$, and the solvent was evaporated. The remaining oil was purified by flash chromatography (AcOEt/hexane 1:3) to obtain 4.74 g of a dark green oil that was used without further purification.

(3-Nitrobenzyl)carbamic Acid 9*H*-Fluoren-9-yl Methyl Ester (7). To a solution of 5.32 g (28.2 mmol) of 3-nitrobenzylamine hydrochloride and 24 mL (133 mmol) of diisopropylethylamine in 200 mL of dichloromethane was added a solution of 7.29 g (28.2 mmol) of Fmoc-Cl in 50 mL of dichloromethane. After stirring overnight at room temperature, the solution was extracted 3 times with 10% HCl. The organic phase was washed with sat. $NaHCO_3$, then water and brine. After drying over $MgSO_4$ and evaporation of the solvent, 10.7 g (quant.) of a white solid were obtained. Mp 152−153 °C. ^{1}H NMR (DMSO-d_6, 400 MHz): δ 8.13−8.11 (m, 2 H), 8.01 (t, J = 6.1 Hz, 1 H), 7.89 (d, J = 7.5 Hz, 2 H), 7.70−7.61 (m, 4 H), 7.42 (t, J = 7.4 Hz, 2 H), 7.34−7.30 (m, 2 H), 4.38 (d, J = 6.8 Hz, 2 H), 4.32 (d, J = 6.1 Hz, 2 H), 4.24 (t, J = 6.7 Hz, 1 H). ^{13}C NMR (DMSO-d_6, 100 MHz): δ 156.3, 147.7, 143.7, 142.1, 140.7, 133.7, 129.8, 127.5, 126.9, 125.0, 121.7, 121.5, 120.0, 65.4, 46.7, 43.0. HRMS (MALDI, DHB) *m*/*z* (M + Na)$^+$ calcd 397.1159, found 397.1160.

(3-Aminobenzyl)carbamic Acid 9*H*-Fluoren-9-yl Methyl Ester (8). In 500 mL of a 2:1 mixture of ethanol and 1,4-dioxane 10.7 g (28.6 mmol) of **7** were dissolved. After addition of 100 mg of PtO_2 under argon, the atmosphere was changed to H_2 (1 bar). After 2 h of vigorous stirring, the catalyst was removed by filtration over Celite. After evaporation of the solvent, 9.9 g (quant.) of an off white solid were obtained. Mp 142−143 °C. ^{1}H NMR (DMSO-d_6, 400 MHz): δ 7.89 (d, J = 7.5 Hz, 2 H), 7.75 (t, J = 6.1 Hz, 1 H), 7.71 (d, J = 7.4 Hz, 2 H), 7.44−7.40 (m, 2 H), 7.35−7.31 (m, 2 H), 6.94 (t, J = 7.7 Hz, 1 H), 6.46 (s, 1 H), 6.43 (d, J = 7.9 Hz, 1 H), 6.38 (d, J = 7.5 Hz, 1 H), 5.00 (s, 2 H), 4.31 (d, J = 6.9 Hz, 2 H), 4.22 (t, J = 6.9 Hz, 1 H), 4.05 (d, J = 6.1 Hz, 2 H). ^{13}C NMR (DMSO-d_6, 100 MHz): δ 156.2, 148.5, 143.8, 140.6, 140.2, 128.6, 127.5, 127.0, 125.1, 120.0, 114.4, 112.4 (2 isochronous signals), 65.3, 46.7, 44.0. HRMS (MALDI, DHB) *m*/*z* (M + Na)$^+$ calcd 367.1417, found 367.1417. Elemental analysis $C_{22}H_{20}N_2O_2$, calcd: C, 76.72; H, 5.85; N, 8.13; O, 9.29. Found: C, 76.82; H, 5.94; N, 8.04; O, 9.46.

(3-{3-[(9*H*-Fluoren-9-ylmethoxycarbonylamino)methyl]phenylazo}-phenyl)acetic Acid *tert*-Butyl Ester (9). A solution of 4.74 g of **5** in 200 mL of glacial acetic acid was added to a solution of 7.36 g (21.4 mmol) of **8** in 200 mL of glacial acetic acid and stirred for 48 h at room temperature. The solvent was removed in vacuo, and the remaining gum purified by flash chromatography (AcOEt/hexane 1:3) to obtain 6.74 g (57%) of a bright orange solid. Mp 64−66 °C. ^{1}H NMR ($CDCl_3$, 500 MHz): δ 7.84−7.80 (m, 4 H), 7.75 (d, J = 7.4 Hz, 2 H), 7.60 (d, J = 7.4 Hz, 2 H), 7.49−7.45 (m, 2 H), 7.41−7.37 (m, 4 H), 7.30 (m, 2 H), 5.20 (bs, 1 H), 4.49−4.47 (m, 4 H), 4.24 (t, J = 6.9 Hz, 1 H), 3.63 (s, 2 H), 1.45 (s, 9 H). ^{13}C NMR ($CDCl_3$, 125 MHz): δ 170.5, 156.5, 152.9, 152.7, 143.9, 141.3, 139.6, 135.9, 132.0, 130.0, 129.5, 129.2, 127.7, 127.1, 125.0, 123.5, 122.4, 121.8, 121.4, 120.0, 81.1, 66.8, 47.3, 44.9, 42.4, 28.1. HRMS (MALDI, DHB) *m*/*z* (M + Na)$^+$ calcd 570.2363, found 570.2371. Elemental analysis $C_{34}H_{33}N_3O_4$, calcd: C, 74.57; H, 6.07; N, 7.67; O, 11.69. Found: C, 74.47; H, 6.18; N, 7.56; O, 11.73.

(3-{3-[(9*H*-Fluoren-9-ylmethoxycarbonylamino)methyl]phenylazo}-phenyl)acetic Acid (10). To a solution of 6.74 g (12.3 mmol) of **9** in 500 mL of dichloromethane was added 50 mL of trifluoroacetic acid. After stirring for 36 h, 200 mL of water was added and the organic layer was separated and washed with water and brine. After drying over $MgSO_4$, the solvent was removed to obtain 5.87 g (97%) of an

(49) Goddard, T. D.; Kneller, D. G. *SPARKY 3*, version 3.106; University of California: San Francisco.
(50) Scott, W. R. P.; Hünenberger, P. H.; Tironi, I. G.; Mark, A. E.; Billeter, S. R.; Fennen, J.; Torda, A. E.; Huber, T.; Krüger, P.; van Gunsteren, W. F. *J. Phys. Chem. A* **1999**, *103*, 3596−3607.
(51) van Gunsteren, W. F.; Billeter, S. R.; Eising, A. A.; Hünenberger, P. H.; Krüger, P.; Mark, A. E.; Scott, W. R. P.; Tironi, I. G. *Biomolecular Simulation: The GROMOS96 Manual and User Guide*; Verlag der Fachvereine (vdf): Zürich, 1996.
(52) Berendsen, H. J. C.; Postma, J. P. M.; van Gunsteren, W. F.; Hermans, J. *Intermolecular Forces*; Reidel: Dordrecht, 1981; pp 341−342.

orange-brown solid. Mp 168−169 °C. ^{1}H NMR (DMSO-d_6, 400 MHz): δ 12.43 (bs, 1 H), 8.00 (t, J = 6.1 Hz, 1 H), 7.89 (d, J = 7.5 Hz, 2 H), 7.80−7.77 (m, 4 H), 7.72 (d, J = 7.5 Hz, 2 H), 7.58−7.53 (m, 2 H), 7.49−7.39 (m, 4 H), 7.33−7.30 (m, 2 H), 4.38 (d, J = 6.8 Hz, 2 H), 4.33 (d, J = 6.1 Hz, 2 H), 4.25 (t, J = 6.8 Hz, 1 H), 3.74 (s, 1 H). ^{13}C NMR (DMSO-d_6, 100 MHz): δ 172.4, 156.3, 151.9, 151.8, 143.8, 141.3, 140.7, 136.5, 132.6, 130.1, 129.3, 129.2, 127.5, 126.9, 125.0, 123.0, 121.5, 121.3, 120.4, 120.0, 65.3, 46.7, 43.4, 40.2. HRMS (MALDI, DHB) m/z $(M + Na)^+$ calcd 514.1737, found 514.1731.

Acknowledgment. We thank Dr. Marc-Olivier Ebert and Prof. Bernhard Jaun for their help with the interpretation of the NMR data.

Supporting Information Available: Tables with chemical shifts for *cis*-**1b** and list of NOE resonance assignments. This material is available free of charge via the Internet at http://pubs.acs.org.

JA0442567